PS Delineating Previously Field-Mapped Hydrocarbon Seepage using Medium Resolution Satellite Imagery in the Zagros Fold & Thrust Belt*

Mike Oehlers[1] and Ross Smail[2]

Search and Discovery Article #42501 (2020)**
Posted February 17, 2020

*Adapted from poster presentation given at 2019 AAPG Hedberg Conference, Hydrocarbon Microseepage: Recent Advances, New Applications, and Remaining Challenges, Houston, Texas, United States, June 18-20, 2019
 DOI:10.1306/42501Oehlers2020

[1]Tectosat Ltd, Reigate, Surrey, UK (mike.oehlers@Tectosat.com)
[2]Getech Ltd, London, UK (ross.smail@getech.com)

Abstract

The search for liquid hydrocarbons using visual indicators of surface seepage has a history dating back to the Mesopotamian/Babylonian Civilisations, around 4000BC, when the resource was used for fueling lamps and providing pitch for waterproofing boats. It therefore seems prescient that we have chosen the Zagros Fold & Thrust belt as a natural laboratory to continue the search for expressions of migrating Hydrocarbons. Our research focuses on providing a regional screening tool to assess whether a combination of medium resolution Landsat, ASTER and Hyperion data can be used to discriminate seepage signatures emanating from the foothills and frontal fold-thrust domains of the prolific Zagros Hydrocarbon Province. We would like to illustrate the utility of such a technique by mapping a number of previously field-mapped seepage locations and impregnation types (i.e. oil, gas, bitumen, sulphur spring, gach-e-turush) compiled by BP Geologists in the 50's and 60's and since published on readily accessible geological maps. Each location has been mapped geologically – structure and local stratigraphy – at 1:50,000 scale using publicly available and free to acquire Landsat OLI and SRTM data to characterise each locality. Stratigraphic units mapped by BP have been re-mapped at greater scale to provide geological context for our efforts at discriminating the local seepage types. Understanding the local geology will help to understand the migration constraints both structurally and geochemically. We have used a combination of surface seepage indicators that have been widely published since the advent of medium resolution multispectral sensors in the early 90's and as such, Schumacher's (1996, and subsequently by many others) paper describes the main types of anomaly that can be expected and detected by remote sensing applications. These relate to spectrally resolving the alteration of clays to Kaolinite, redox-related ferric-ferrous red bed bleaching, and lastly carbonate, gypsum and silica precipitation. We have not considered vegetation anomalies in this location due to the sparse vegetation cover. We have used a range of techniques including atmospherically corrected and orthorectified image processing, ASTER-derived band ratios (from previously published sources), relative absorption depth ratios, focused PCA and multi-temporal image stacking that can then be semiautomated in ArcGIS to provide anomalous spectral signatures relating to the 5 classes of alteration commonly reported, as mentioned above. We then "stack" our results to illustrate how alteration mineral assemblages relate to the different seepage styles mapped on the ground. Spectral Library (primarily USGS) signatures have been used as we have had no access to the field samples. At present, we have not yet used more advanced remote

sensing techniques involving spectral angle mapping, mixture-tuned match filtering/pixel-unmixing or other statistical approaches as we do not have field samples to calibrate to. While we realise the potential limitations of this approach, our initial aim is to provide a rapid and semi-automated hydrocarbon province/domain screening tool that locates likely seepage clusters that warrant further appraisal, using Very High Resolution imagery (such as WV3) combined with targeted field verification and sample collection. Our poster shows our preliminary results and how these might provide a useful regional screening tool, using our semi-automated processing workflow, based on the 10 sites in the Zagros Mountains. The results indicate that the seepage impregnations mapped in the field 70 years ago can be readily recognised on the imagery, but that others have no discernible signature, albeit at the resolution that the data we have used provides. We hope in the near future to augment our results with additional study using more discriminating remote sensing techniques and Hyperion and WV3 data in this region and others where access to ground truthing and sampling allows a more fully inclusive investigation.

References Cited

Bahroudi and Koyi, 2004. Tectono-sedimentary framework of the Gachsaran Formation in the Zagros foreland basin. Marine and Petroleum Geology, 21, p. 1295–1310.

Crosta, A. P., De Souza Filho, C. R., Azededo, F. and Brodie, C., 2003. Targeting key alteration minerals in epithermal deposits in Patagonia, Argentina, using ASTER imagery and principal component analysis. International Journal of Remote Sensing, 24, Vol 21, p. 4233-4240.

Schumacher, D., 1996. Hydrocarbon-induced alteration of soils and sediments, in D. Schumacher and M. A. Abrams, eds., Hydrocarbon migration and its near- surface expression: AAPG Memoir 66, p. 71–89.

Delineating previously Field-mapped Hydrocarbon Seepage using Medium Resolution Satellite Imagery in the Zagros Fold & Thrust belt

Delineating previously Field-mapped Hydrocarbon Seepage using Medium Resolution Satellite Imagery in the Zagros Fold & Thrust belt

Mike Oehlers (1) and Ross Smail (2)
(1) Tectosat Ltd, Reigate, Surrey, UK, mike.oehlers@Tectosat.com
(2) Getech Group plc, Leeds, UK, ross.smail@getech.com>
Full resolution poster download from:
https://www.exprodat.com/featured/downloads/indentifying-onshore-seeps-poster/

1. Abstract

The search for liquid hydrocarbons using visual indicators of surface seepage has a history dating back to the Mesopotamian/Babylonian Civilisations, around 4000BC, when the resource was used for fuelling lamps and providing pitch for waterproofing boats. It therefore seems prescient that we have chosen the Zagros Fold & Thrust belt as a natural laboratory to continue the search for expressions of migrating Hydrocarbons.

Our research focuses on providing a regional screening tool to assess whether a combination of medium resolution Landsat, ASTER and Hyperion data can be used to discriminate seepage signatures emanating from the foothills and frontal fold-thrust domains of the prolific Zagros Hydrocarbon Province. We would like to illustrate the utility of such a technique by mapping a number of previously field-mapped seepage locations and impregnation types (i.e. oil, gas, bitumen, sulphur spring, gach-e-turush) compiled by BP Geologists in the 50's and 60's and since published on readily accessible geological maps.

Each location has been mapped geologically – structure and local stratigraphy – at 1:50,000 scale using publicly available and free to acquire Landsat OLI and SRTM data to characterise each locality. Stratigraphic units mapped by BP have been re-mapped at greater scale to provide geological context for our efforts at discriminating the local seepage types. Understanding the local geology will help to understand the migration constraints both structurally and geochemically.

We have used a combination of seepage indicators that have been widely published since the advent of medium resolution multispectral sensors in the early 90's and as such, Schumacher's (1996, and subsequently by many others) paper describes the main types of anomaly that can be expected and detected by remote sensing applications. These relate to spectrally resolving the alteration of clays to Kaolinite, redox-related ferric-ferrous red bed bleaching, and lastly carbonate, gypsum and silica precipitation. We have not considered vegetation anomalies in this location due to the sparse vegetation cover.

We have used a range of techniques including atmospherically corrected and orthorectified image processing, ASTER-derived band ratios (from previously published sources), relative absorption depth mapping, focussed PCA and multi-temporal image stacking that can then be semi-automated in ArcGIS to provide anomalous spectral signatures relating to the 5 classes of alteration commonly reported, as mentioned above. We then "stack" our results to illustrate how alteration mineral assemblages relate to the different seepage styles mapped on the ground.

Spectral Library (primarily USGS) signatures have been used as we have had no access to the field samples. At present, we have not yet used more advanced remote sensing techniques involving spectral angle mapping, mixture-tuned match filtering/pixel-unmixing or other statistical approaches as we do not have field samples to calibrate to.

While we realise the potential limitations of this approach, our initial aim is to provide a rapid and semi-automated hydrocarbon province/domain screening tool that locates likely seepage clusters that warrant further appraisal, using Very High Resolution imagery (such as WV3) combined with targeted field verification and sample collection.

Our poster shows our preliminary results and how these might provide a useful regional screening tool, using our semi-automated processing workflow, based on the 10 sites in the Zagros Mountains. The results indicate that the seepage impregnations mapped in the field 70 years ago can be readily recognised on the imagery, but that others have no discernible signature, albeit at the resolution that the data we have used provides. We hope in the near future to augment our results with additional study using more discriminating remote sensing techniques and Hyperion and WV3 data in this region and others where access to ground truthing and sampling allows a more fully inclusive investigation.

Figure 1, below: Location of the study areas (red outlines) within the Zagros Fold-Thrust Belt

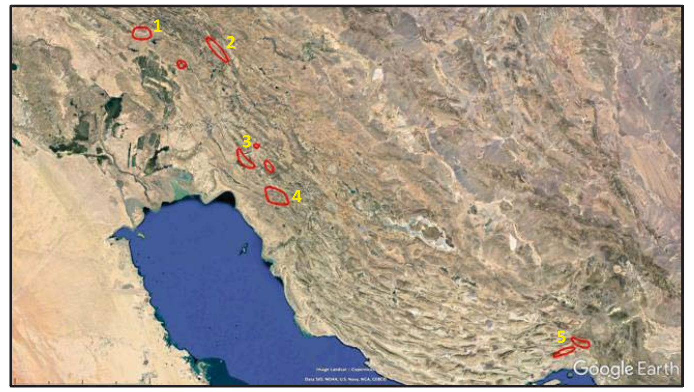

2. Introduction

Getech and Tectosat have, since summer 2018, began a research pilot project to explore the viability of Medium and Very High (VHR) resolution satellite imagery to map isolate surface expressions of micro- and macro-seepage. The project aims to provide a semi-automated processing chain to highlight areas using medium resolution ASTER imagery for more detailed VHR follow up with WorldView 3 (WV3) data.

This poster presents initial results from our pilot project using ASTER 15/30/60m resolution VNIR, SWIR and TIR data over the Zagros Mountains, the uplifted domain that forms part of the Zagros-Mesopotamian Foreland, Fold and Thrust Belt in the northern Middle East. The foothills and the foreland basin represent the largest petroleum province in the world and was mapped in detail by many geologists in the first half of the 20th Century. BP in particular mapped the region and the maps are published and available for study from the Geological Society of London. In addition to standard geological attributes, the locations of surface seepage, springs, impregnations and encrustations of hydrocarbon-related fluids were mapped.

Our intention was to test whether ASTER data could be used to screen large areas using semi-automated processing workflows and the premise was to investigate whether the ASTER data could indeed record and isolate the signatures of surface hydrocarbon seepage that have been widely published in the academic press since the advent of medium resolution satellite images in the 1990's. We have used the locations of the mapped seepage sites on the BP maps as calibration points to test whether the mineral alteration and precipitation products predicted by this early research can be mapped using the ASTER data. In this poster, we do not attempt to review in detail the history or development of the techniques previously published. As such, our aims at this stage are two-fold:-

- Can we use ASTER to map seepage signatures, using existing mapping as calibration?
- Can we develop a semi-automated toolkit to process the imagery required?

3. Methodology.

The basis for the processing chain is laid out below.

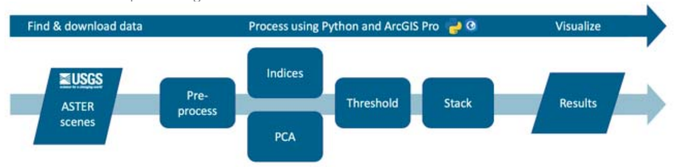

Figure 2, above: Workflow showing the processing chain

The desire was to automate the processing as far as was possible so that a standard set of outputs could be generated for any given area. An ArcGIS Pro Python toolbox was developed, including the following principal scripts:

- Pre-process ASTER dataset:

Converts the source HDF file into a single multiband TIFF image with appropriate metadata, correcting alignment issues between VNIR and SWIR.

- Create index products:

Creates a set of band index images highlighting specific mineral species, from the single multiband TIFF image.
Thresholds the images at the 95th and 99th percentiles

- Create PCA products:

Creates a set of PCA images targeting specific mineral species (as per Crósta et al, 2003), from the single multiband TIFF image.
Thresholds the images at the 95th and 99th percentiles

- Stack products:

Stacks (sums) the thresholded images ready for visualization

The entire workflow takes approximately 15 mins/image to complete using a laptop computer. The separation of steps allows additional masking and extraction workflows to be executed as required. A more detailed description of the products is illustrated below.

Figure 3: below: ArcGIS Pro Python toolbox and the 4 automated processing steps

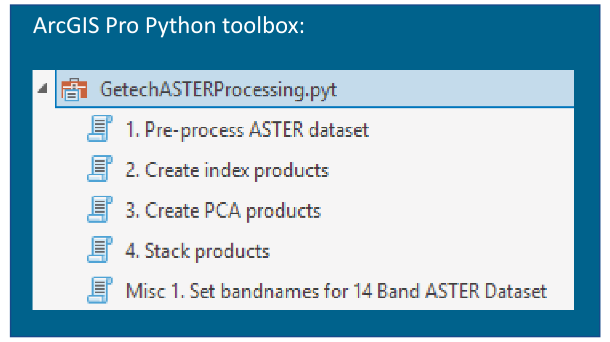

- Band index generation – concepts

Band indices are designed to highlight specific mineral species, based on their spectral characteristics – i.e. their particular reflection or absorption features.

To take a simple example, ferrous minerals appear red to the naked eye as they reflect more red light than they reflect green light. A band index (or ratio) created by dividing a red band image by a green band image will highlight areas that reflect more red light than green light – if ferrous minerals are present at the surface then the pixels in which they occur will appear brighter in the band index image.

The same logic can be applied to develop band indices for other mineral species with particular spectral characteristics in the wavelengths covered by the sensor in use, with more complex multi-band combinations being designed to attempt to discriminate particular mineral species from those with similar spectral characteristics.

- PCA – concepts

Principal component analysis is a technique that can be used to reduce the dimensionality of a multi-band image dataset by removing redundant information. Each derived principal component image represents part of the variance of the original image dataset, with the first principal component image containing the greatest part of the variance, the second the second greatest part, etc.

PCA can be combined with the concepts used in band index design and used to generate principal component images for selected band combinations that target specific mineral species. A particular variant of this technique is referred to the Crósta technique, after its developer, Alvaro Crósta, who designed the set of band combinations used in this study. Having created principal component images using a specific combination – e.g. ASTER bands 1, 4, 6 and 7, for targeting Kaolinite – the eigenvector matrix is examined to identify which of the principal components contains the target spectral information, and that image is then used to represent the relative abundance of the target mineral species (see Crósta et al 2003 for further detail).

The scripts developed for this project attempt to automate the examination of the eigenvector matrix and the selection of the correct principal component, but in cases where there could be confusion, all possible candidate principal components are output.

We have used widely accepted band indices and PCAs in this study.

Table 1, below: Band index products

Target mineralogy	ASTER band combination
Carbonate	(Band 7 + Band 9)/Band 8
Ferrous	Band 1/Band 2
Gypsum	Band 4/(Band 9 + Band 6)
Montmorillonite	(Band 4 + Band 6)/Band 7
Quartz-rich	Band 14/Band 12

PCA products:

Target mineralogy	PCA band combination
Illite	Bands 1, 3, 5, 6
Kaolinite and Smectite	Bands 1, 4, 6, 9
Kaolinite	Bands 1, 4, 6, 7

Following examination of published research, we decided to concentrate on the most prominent reported alteration and precipitation products common to most of the existing work:-

- Alteration of clays to kaolinite
- Redox-related ferric-ferrous red bed bleaching
- Precipitation of Gypsum, carbonate and silica

As much of the region is sparsely vegetated, much on permeable and porous limestone-karst topography, we decided not to look at vegetation anomalies. The few excessively vegetated (mountainous) forests and more extensive lowland farmed areas were masked out.

4. Results

The Zagros Foreland Fold and Thrust Belt (FFTB) presents a fine laboratory for remote sensing as a consequence of its aridity and climate, allowing frequent imaging of exposed lithology and geological structure at virtually any time of year. We have chosen three domains of the FFTB that display multiple surface impregnations and active/inactive seepage and spring phenomena.

The domains themselves are controlled by the Neogene to Present tectonism reacting with pre-existing palaeo-geographic domains with coeval and subsequent development of Neogene (mostly Miocene) evaporite basins. These sub-basinal domains developed thick evaporitic units known as "Gachsaran" and comprise, in decreasing amounts, evaporites, clays, limestones and shales. This unit provides a regionally important décollement surface and mineralogy that reacts enthusiastically with locally sourced migrating hydrocarbon fluids. Our calibration locations therefore fall within the Dezful and Qeshm Evaporite Basin domains mentioned by Bahroudi and Koyi, (2004).

It should be noted that several of the test areas were subsequently abandoned as the seepage localities had been submerged due to the construction of dams or were unsuitable geologically. We have chosen 6 locations to highlight in this poster: Rud-e-Kharkeh (1), Ab-e-Bhazuft (2), Kuh-e-Kaviz (3), Gachsaran (4), all in the Dezful Embayment Evaporite Basin, Kush Kun and Sarzeh Rud (5), both in the Qeshm Evaporite Basin; numbers in brackets refer to locations shown in Figure 1.

In terms of interpretation procedure, each location was mapped using Landsat and SRTM DEM imagery to provide some detailed geological background to each locality. The detail consisted of re-mapping at 1:50,000 scale, using the previous 1:250,000 scale BP maps as a guide. Each location was then examined using the products highlighted above (section 3) by first laying over a Montmorillonite and then Illite Clay 95/99% map and then overlaying that with our Kaolinite 95/99% maps to show whether alteration from one clay state to the other could be indicated. The next step was to overlay gypsum, carbonate, silica and ferric 95/99% maps to see if evidence of other potentially seepage related alteration or precipitation indicators were present. The mapped geology provided context both stratigraphically and structurally. We provide examples from these 6 locations below.

The following figures show our initial results around the AOIs mentioned above. The colour codes for all the subsequent figures is the same and are set out in the table below. Likewise, each figure shows standard geological symbols to show anticlines/synclines, thrust/normal faults. Stratigraphic boundaries (derived from Landsat data at 1:50,000 scale) are shown in green.

Table 2, below: explanation of the colours used in all figures.

1 mineral index pixel		Carbonate (95/99% Threshold)	
2 mineral index pixels		Gypsum	
3 mineral index pixels		Ferrous	
4 mineral index pixels		Illite	
5 mineral index pixels		Kaolinite	
6 mineral index pixels		Kaolinite-Smectite	
7 mineral index pixels		Montmorillonite	
8 mineral index pixels		Quartz-rich	

The locations of the seepage indicators mapped by BP are shown on the maps as red circles. We have found that the general accuracy of the topographic information and the absolute locations of the BP geology maps to be of only moderate accuracy: compared to modern satellite images (~2017/8) some of the geographical features are displaced by up to 1 Km, so the accuracy of the seep locations could also be affected.

4.1 : Rud-e-Kharkeh (Location Number 1, Figure 1)

The Rud-e-Kharkeh AOI is located in the North of the Dezful Embayment and lies on the margin of the Dezful Evaporite Basin, the folds forming the foothills of the Zagros FFTB. The BP geological maps show a cluster of seeps on the southern limb of a small anticline cored by Oligo-Miocene Asmari Lst., a competent carbonate sequence that underlies the mobile and ductile Fars Group (now Fars Formation). The folds are thrust cored, but the back limb of the fold and the fold lying immediately to the north-east are separated by a series of smaller anticlines, synclines and emergent thrusts that indicate smaller scale accommodation structures between the folds and point to a more complex subsurface structural fault network.

The Fars Fm comprises evaporites, marls and limestone units and is responsible for disharmonic folding and decollement in overlying units, commonly offsetting the axes of deeper anticlinal cores and thrust fault geometries with the observed surface anticlines. The unit also hosts much if not all of the "Gach-e-Turush" or self-igniting flames resulting from an association of oxidizing petroleum seep, gypsum, jarosite, sulphuric acid, and sulphur. The resulting sulphur produce sulphur streams and in addition to the Gach-e-Turush deposition, may also be associated with asphalt impregnations and bitumen seepage. All of these phenomena are common in this location and at the Gachsaran location, described in the next section.

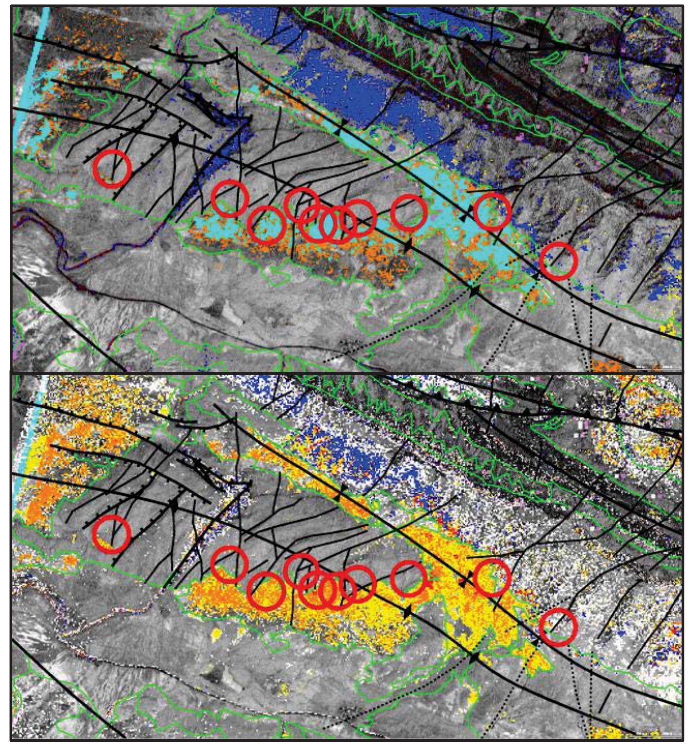

Figure 4: Top – 8 indices coloured individually; below – "stacked" indices for Rud-e-Kharkeh

Figure 4 illustrates the result from the AOI; the top image shows the results of the thresholded mineral mapping (see Table 2 for colour coding) and the lower image the "stacking" results. Warmer colours (here including magenta/purple) indicate higher concentrations of two or more constituent minerals in the same location, such that a purple coloured pixel would include high concentrations of all 8 mapped minerals.

The red circles superimposed on the images show locations (bearing in mind the inaccuracies noted above) of seepage mapped by BP geologists. In this location, most of the seepage comprises asphalt impregnations and active asphalt seeps, together with a few sulphur streams. Our stacking map seems to show a good relationship between mapped seeps and high-value stacked anomaly, although the mapped seeps at left (west) and lower right (east) show some but not much anomaly in the immediate area. On the anticline to the NE, three other seepage sites were mapped, but these do not show any noticeable anomaly. However, immediately SW, two localities previously mapped do show anomaly, but our mapped stacks are offset by 750m – possibly due to base-mapping defects.

4.2 : Gachsaran (Number 4, Figure 1)

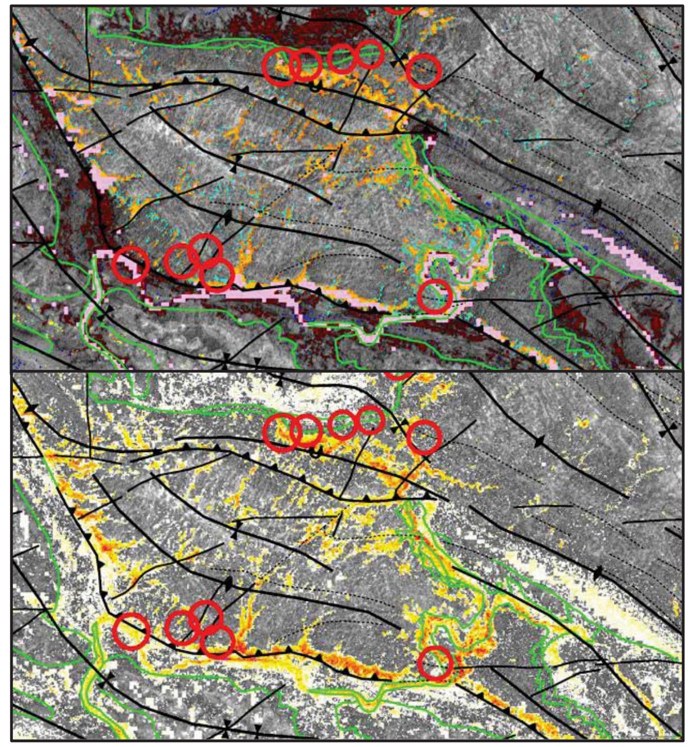

Figure 5: Top – 8 indices coloured individually; below – "stacked" indices for Gachsaran

Gachsaran lies in southern part of the Dezful Embayment and is the type locality for the Gachsaran Formation, formerly part of the Fars Group. The main facets of the geology here are very similar to that in the north of the embayment (i.e. Rud-e-Karkeh) and the same sequences are deformed by the same style of structure although décollement and disharmonic folding are more common in the basinal setting in Gachsaran than the marginal location at Rud-e-Karkeh. Two concentrations of seep were mapped by BP – a group of 5 in the north – which are all Gach-e-Turush style seeps – and another set in the south of the image (sulphur springs) developed along the thrust front. The seeps match closely with our mapped stacks and suggest further anomalies may lie along the entire thrust front.

4.3 : Ab-e-Bhazuft (Number 2, Figure 1)

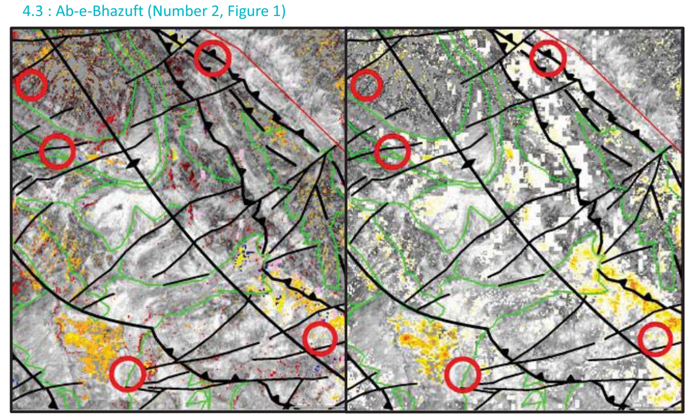

Figure 6: Left – 8 indices coloured individually; right – "stacked" indices for Ab-e-Bhazuft

The Ab-e-Bhazuft images show that in this area, very few of the mapped surface seeps were picked up by the processing we applied. There are one or two near misses, but generally, nothing was picked up in this domain. The Gachsaran Formation is absent here so structural style is different with less disharmonic folding and more conventional fault-bend folding with no evaporites to glide over or supply sulphur for springs and Gach-e-Turush.

4.4 : Kuh-e-Kaviz (Number 3, Figure 1)

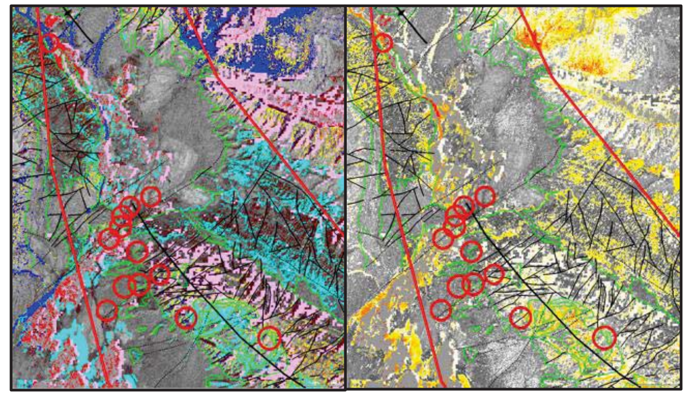

Figure 7: Left – 8 indices coloured individually; right – "stacked" indices for Kuh-e-Kaviz

As in the Ab-e-Bhazuft AOI, the Kuh-e-Kaviz area shows few previously mapped seep sites have been captured by the processing. As with the other domains above this may be due to the small size of the actual seepage sites or due to the spectral resolution of the ASTER data. Additionally in this area, much of the low-lying terrain is intensely farmed and the masking process has occluded some areas and created some edge effects , so the relationships are unclear.

4.5 : Kush Kun and Sarzeh Rud (Number 5, Figure 1)

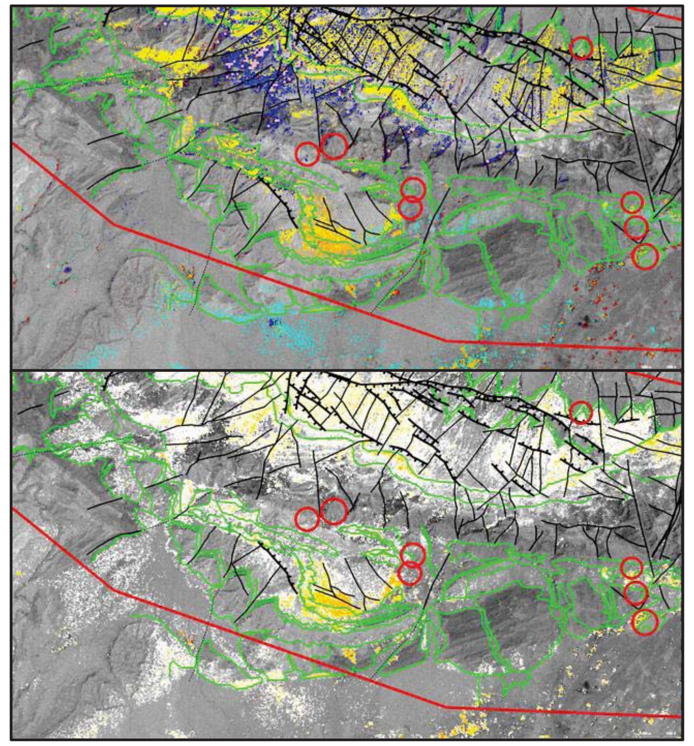

Figure 8: Top – 8 indices coloured individually; below – "stacked" indices for Kush Kun & Sarzeh Rud

The Kush Kun and Sarzeh Rud areas are the furthest south we have reviewed. The area lies within the Qeshm Evaporite basin, sandwiched between the Fars Range (no Gachsaran Fm evaporite) and the Makran Sedimentary Prism. Unlike the Dezful Embayment Evaporite Basin, the domain doesn't contain thick Gachsaran Fm (formerly the "Lower Fars Group") and the structural style is more like the more marginal Ab-e-Bhazuft and Kuh-e-Kaviz domains, lacking décollement surfaces and more controlled by fault bend or fault propagation fold styles.

The Kush Kun structure (Figure 8) lies just to the south of the main boundary fault of the Zagros Mountains, where it joins with the Dibba Fault Zone that separates the Zagros from the Makran accretionary prism. Fault splays from the main fault have bought up Palaeozoic and Infra-Cambrian Salt within the structure and hence the faults provide conduits for an seeping hydrocarbons.

There are several clusters of previously mapped seeps over the structure – a set developed along a splay from the aforementioned boundary faults, for which there is scant record spectrally and a further set, mostly oil impregnations, lying en-echelon with a tear fault formed in the frontal limb of the structure, for which there are several anomalies picked up by our mapping (Figure 8).

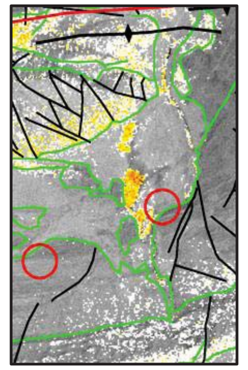

Figure 9: Left - Stacked anomalies developed south of major fold.

Further to the south-west, some isolated seep locations lie south of the Sarzeh Rud area. The example in the central north-east of the image, left, shows a tight group of stacked mineral abundances that coincide with a mapped seep. Although in this image the red circle is displaced to the E/SE, the map shows it straddling a stream, but the map accuracy is poor and the anomalies lie a stream on the Landsat and ASTER imagery.

The high values here may relate to increased vegetation in moister soils ponded by several outcrop ridges but also may relate to the thermal and sulphur spring that is mapped here by the BP geological team. An adjacent sulphur spring - lying to the west – shows no signs of anomaly.

5. Conclusions

We have the following comments and observations following this initial phase of research into seepage and mapping signatures using ASTER data:-

- To date, we have only attempted basic processing– no pixel unmixing, cross-talk etc
- We have had no field-based spectral control
- Some indices are strongly affected by shadows
- Lithology can mask the effects of some seepage if clay rich
- Water bodies/streams are bright in many of the indices and many seeps are associated with water tables interacting with stream beds
- Larger water bodies can dominate the spectral responses and need masking
- Some previously mapped seeps may be too small to map with 15/30/60m pixels
- Better masking out of arable/vegetated domains needed
- The automation of the processing has been a success and many images can be processed quickly once chosen
- Mapping the geology (structural and sedimentological) at 1:50,000 scale or better is essential for context
- The method has shown anomalies over or very close to previously mapped seepage but many of the mapped seeps show no alteration/precipitation anomalies using the ASTER data: out of 91 seeps mapped by BP, we found anomalies (95% threshold level) over or close in 29 locations: ~ 32%. But we treat these with caution as lithological association may exert more control than specific seep-related anomaly
- Hyperion data will be explored to review whether it provides a significant increase in spectral resolution over ASTER to complete this phase of the project
- VHR imagery such as WorldView3 will be used in next phase to assess its utility alongside field-based spectra, which should be a necessity in any attempt to map seepage

Acknowledgments

Ross Smail and Mike Oehlers would like to thank Getech and Tectosat respectively for providing materials and opportunity to present these initial results. Thanks are also due to the Graphics (Jules Cullen) and Review teams at Getech, who kindly spent time editing and producing the poster. Lastly, thanks are also offered to AAPG Hedberg Research for selecting us to present at the conference and to the work that goes into driving a successful conference and workshop.

References

Bahroudi and Koyi, 2004. Tectono-sedimentary framework of the Gachsaran Formation in the Zagros foreland basin. Marine and Petroleum Geology, 21, p. 1295–1310 .
Crosta, A. P., De Souza Filho, C. R., Azededo, F. and Brodie, C., 2003. Targeting key alteration minerals in epithermal deposits in Patagonia, Argentina, using ASTER imagery and principal component analysis. International Journal of Remote Sensing, 24, Vol 21, p. 4233-4240
Schumacher, D., 1996. Hydrocarbon-induced alteration of soils and sediments, in D. Schumacher and M. A. Abrams, eds., Hydrocarbon migration and its near- surface expression: AAPG Memoir 66, p. 71–89.

Suggested Reading

W. K. Link. 1952. Significance of Oil and Gas seeps in world oil exploration. AAPG Memoir 36, p. 1505–1540.
M. J. Abrams, J. E. Conel, H. R. Lang, and H. N. Paley, 1985. eds.. The Joint NASA/Geosat Test Case Project: final report: AAPG Special Publication, pt. 2, v. 2, p. 11-1–11-28.
R. H. Clarke and R. W. Cleverly, 1991. Petroleum seepage and post-accumulation migration. Geological Society, London, Special Publications 1991; v. 59; p. 265-271
Donald F. Saunders, K. Ray Burson, and C. Keith Thompson, 1999. Model for Hydrocarbon Microseepage and Related Near-Surface Alterations, AAPG Bulletin, V. 83, No. 1 (January 1999), p. 170–185.
J.M. Ellis, H.H. Davis and J.A. Zamudio, 2001. Exploring for onshore oil seeps with hyperspectral imaging, Oil and Gas Journal, 99.37, p 49-58
F. van der Meer,* P. van Dijk, H. van der Werff and H. Yang, 2002. Remote sensing and petroleum seepage: a review and case study. Terra Nova, 14, p 1–17
H. M. A. Van Der Werff, M. F. Noomen, M. Van Der Meijde & F. D. Van Der Meer, 2007. Remote sensing of onshore hydrocarbon seepage: problems and solutions. Teeuw, R. M. (ed.) Mapping Hazardous Terrain using Remote Sensing. Geological Society, London, Special Publications, 283, 125–133.
G. Zhang, L. Zou, X. Shen, S. Lu, C. Li, and H. Chen, 2009. Remote sensing detection of heavy oil through spectral enhancement techniques in the western slope zone of Songliao Basin, China. AAPG Bulletin, v. 93, no. 1 (January 2009), pp. 31–49
S. Salati, F. J. A. van Ruitenbeek, J. B. de Smeth, and F. D. van der Meer, 2014. Spectral and geochemical characterization of onshore hydrocarbon seep-induced alteration in the Dezful embayment, southwest Iran. AAPG Bulletin, v. 98, no. 9 (September 2014), pp. 1837–1857
S. Asadzadeh and C. R. de Souza Filho, 2016. Investigating the capability of WorldView-3 superspectral data for direct hydrocarbon detection. Remote Sensing of Environment 173, p 162–173
S. Khan, S. Rahman, M. Haq and S. Munir, 2016. Hyperspectral Remote Sensing for Detection of Natural Hydrocarbon Seeps. Asian Journal of Multidisciplinary Studies, Vol. 4, Issue 2, February 2016